Effect of Doping Thin Films of Nickel Oxide by Cobalt on The Physical and Chemical Properties

L. Dahbi [a,*], C. Zaouche [b], A. Gahtar [c], C. Maghni [d], S. Seggai [e]

[a]Teacher Education College of Setif, Messaoude Zeghar, Algeria.
[b]Material Sciences Department, Faculty of Science, University of Biskra, 07000 Biskra, Algeria.
[c]Department of biology, Faculty of sciences, University Elchahid Hamma Lakhder, 39000 El Oued, Algeria.
[d]Faculty of Science and Technology, University Mohammed chérif messaadia BP 1553 Souk Ahras 41000, Algeria.
[e]Higher School of Agriculture Sahrian in El Oued, Algeria.

Email : l.dahbi@ens-setif.dz

Received 22 March 2023; Accepted 19 October 2023

Abstract:

The effect of Co doping on optical, structural and electrical properties of deposited $Ni_{1-x}Co_xO$ thin films on glass substrate by spray pyrolysis technique has been studied. The main objective of this research is to study the change of the physical and optical properties of $Ni_{1-x}Co_xO$ thin films that are fabricant to semi-conductor with different doping levels x . These levels are 0 at.%, 2 at.%, 6 at.%, 8 at.% and 10 at.%. The transmission spectra show that the $Ni_{1-x}Co_xO$ thin films have a good optical transparency in the visible region from 64 to 82%. The optical gap energy of the $Ni_{1-x}Co_xO$ thin films varied between 3.58 and 3.66 eV. The urbach energy varied between 388 and 500 meV. However, the $Ni_{0.94}Co_{0.06}O$ thin films have many defects with maximum value of urbach energy. The $Ni_{0.94}Co_{0.06}O$ thin films have minimum value of optical gap energy. The Ni0.94Co0.06O thin films have maximum value of the electrical conductivity which is 0.015 $(\Omega.cm)^{-1}$. The average electrical conductivity of our films is about (0.01 $(\Omega.cm)^{-1}$). XRD patterns of the $Ni_{1-x}Co_xO$ thin films indicate that films are polycrystalline with cubic structure.

Keywords: Nickel oxide, Thin films, Spray pyrolysis technique, Optical gap energy, Urbach energy
DOINumber:10.48047/nq.2023.21.7.nq23077 **NeuroQuantology2023;21(7):883-888**

1. Introduction

Nickel oxide is one of the most important semiconductor materials in the environmental field due to the detecting ability of toxic gases [1]. Nickel oxide (NiO) has a several different applications in the field of pizoelectronic, optoelectronic, environmental and renewable energy such as sensors, fuel cell electrodes, catalysis, thermoelectric devices, dye-sensitized solar cells (DSSCs) and electrochromic material for displays [2–8]. Moreover, it is used to find suitable material with enhanced properties for gas sensing applications for detecting the sensibility in the environment such as NO_x, SO_x, CO, CO_2…, at high temperature. Because of its semiconductor nature with controlling optical transparency and electrical conductivity, finding the form of the applied interaction is significant. However, several studies have been made to find that the NiO have a high optical transparency and good electrical conductivity at various experimental conditions. NiO thin films have a direct band gap ranging from 3.5 to 4.3 eV [9–10].

Nickel oxide is used as thin layers, which can be deposited in several methods, including molecular

beam epitaxy (MBE), electrochemical deposition, pulsed laser deposition (PLD), chemical vapor deposition and spray Sol–Gel methods, spray pyrolysis technique [11–17]. We used the cobalt doped NiO thin films to improve the optical and electrical properties of deposited thin films. This is a metal transition in the periodic table, which was used in the research because of some rare earth material quality due to the increase in the optical band gap energy (broadening).

In this work, we have prepared Co doped NiO thin films by using the spray pyrolysis technique deposition on glass substrate which its temperature is 470 °C. we sprayed this glass substrate for 5 minutes. Co doped NiO thin films were synthesized with different doping levels (0, 2, 6, 8 and 10 at. %) for $Ni_{1-x}Co_xO$. The $Ni_{1-x}Co_xO$ thin films were used to enhance the optical and electrical properties of deposited thin films. However, we have studied the change of the optical, structural and electrical properties of $Ni_{1-x}Co_xO$ thin films that are fabricant to semiconductor.

2. Experimental procedure

$Ni_{1-x}Co_xO$ solutions were prepared by dissolving the nickel acetate ($Ni(CH_3.CO_2)_2.4H_2O$) and cobalt acetate ($Co(CH_3.CO_2)_2.4H_2O$) with 0.5 mol l^{-1}. In this work, we have used a Co doping with various concentrations in the game Co/Ni = 0, 2, 6, 8 and 10 at.% or (x = 0, 0.02, 0.06, 0.08 and 0.10). Then, we have added a drop of HCl to stabilize heating solution. The mixture solution was stirred at room temperature and heated at 40 °C for 2 h to yield a clear and transparent solution. The coating was made 1 day after the precursor was prepared.

The $Ni_{1-x}Co_xO$ samples were prepared by spraying the coating solution onto glass substrate. Its temperature is 470 °C for 5 minutes to obtain a thin film. The prepared $Ni_{1-x}Co_xO$ thin films at different Co doping levels are 0 at.%, 2 at.%, 6 at.%, 8 at.% and 10 at.%. After the deposition of the thin layers, we left substrate to decrease its temperature to the one of the room.

The structural properties of $Ni_{1-x}Co_xO$ thin films were studied by means of X-ray diffraction (XRD Bruker AXS-8D) with CuKa radiation (λ=0.15406 nm) in the scanning range of (1h) which was between 20° and 70°. The optical transmission of the deposited films was measured in the range of (300–900 nm) by using an ultraviolet-visible spectrophotometer (LAMBDA 25) and the electrical conductivity σ was measured by four point methods.

3. Results and discussion

3.1. Structural properties of $Ni_{1-x}Co_xO$ thin films

The structural characterization of the $Ni_{1-x}Co_xO$ thin films is carried out by X-ray diffraction method that is shown in figure 1. XRD spectra indicate that the films exhibit polycrystalline structure that belongs to the cubic type of NiO (JCPDS) No. 73-1519) [18]. Figure 1 shows that the XRD peaks at 37.18° and 42.98° corresponding to (111) and (200) crystal planes respectively, the peaks position was accordant with Abdur Rahman et al. [19]. We observed that the intensity of (111) and (002) peaks increases in thin films with the increasing doping levels x at x=0.10. This information confirmed that the preferred orientation is along to (111) and (002) planes.

However, the film at x=0.10 has higher and sharper diffraction peaks indicating an enhancement of crystallinity with comparison to other films.

The structure information was defined by the diffraction peak angles of the Co doped NiO thin films (see Table 1). The lattice parameter a of Co doped NiO thin films was calculated from XRD patterns by using the following equation [20]:

$$\frac{1}{d_{hkl}^2} = \frac{h^2 + k^2 + l^2}{a^2} \quad (1)$$

Where h, k and l are the Miller indices of the planes. a is the lattice parameter and dhkl is the inter planar spacing. The crystallite sizes G of (111) and (200) planes were calculated according to the Scherer equation [21- 22]:

$$G = \frac{0.9\lambda}{\beta \cos\theta} \quad (2)$$

Where G is the crystallite size, β1/2 is the full width at half-maximum (FWHM), θ is Bragg angle of the diffraction peaks and λ is the X-ray wavelength (λ=0.15406 nm). The variations are shown in Tables 1 and 2.

The variations of the crystallite size and diffraction angle according to (111) and (200) peaks presented in Figure 2 a and b shows the variation of crystallite size and diffraction angle of Co doped NiO thin films as a function of Co doping level. In Figure 2a, we have observed that the diffraction angles of (111) plan decreased with increasing doping levels x from 0.06 to 0.10 (see Tables 1). The crystallite size of (111) plan decreased to minimum value obtained at

x=0.06 (see Tables 1). On the other hand, Figure 2b shows that the diffraction angles of (200) plan decreased then increased and decreased again with increasing doping levels x to reach the maximum value obtained at x=0.10 (see Table 2). But we observed that the crystallite size of (200) plan decreased to minimum value at x=0.06. The decrease of the crystallite size has been indicated by the enhancement of the crystallinity and a-axis orientation of Co doped NiO thin films. These phenomena were observed in [23–27]. This result can be explained by coalescence of the crystallite of the thin films to improve oxygen diffusion [28].

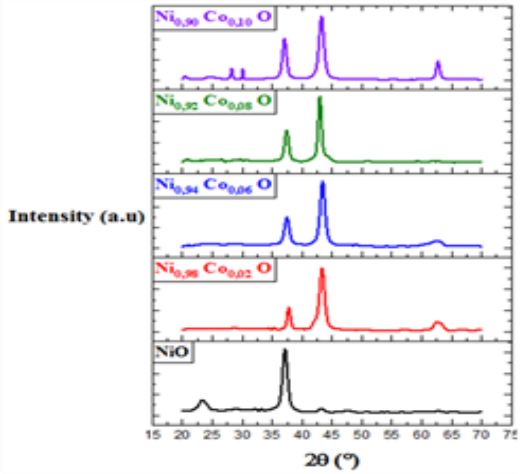

Fig. 1. X-ray diffraction of $Ni_{1-x}Co_xO$ thin films as a function of Co doping level.

Table 1. The structural parameters of Ni1-xCoxO thin film as a function of Co doping level of (111) diffraction peak.

X	2θ(°)	d (nm)	$\beta_{1/2}$ (°)	G(nm)	a(nm)
0	37.2270	0,24145	0.3825	21.9256	0,418209
0.02	37.1870	0,24170	0.6187	13.5535	0,418643
0.06	37.3072	0,24095	0.9335	8.9861	0,417342
0.08	37.2251	0,24146	0.7761	10.8059	0,418230
0.10	36.9526	0,24318	0.6187	13.5442	0,421205

Table 2. The structural parameters of $Ni_{1-x}Co_xO$ thin film as a function of Co doping level of (200) diffraction peak.

x	2θ(°)	d (nm)	$\beta_{1/2}$ (°)	G(nm)	a(nm)
0	42.7956	0,21123	0.3038	28.0978	0,422470
0.0	42.79	0,211	0.461	18.50	0,4224
2	42	24	2	84	83
0.06	43.2319	0,20920	0.7761	11.0152	0,418407
0.08	42.8328	0,21106	0.6187	13.7986	0,422120
0.10	43.2587	0,20908	0.2251	37.9819	0,418161

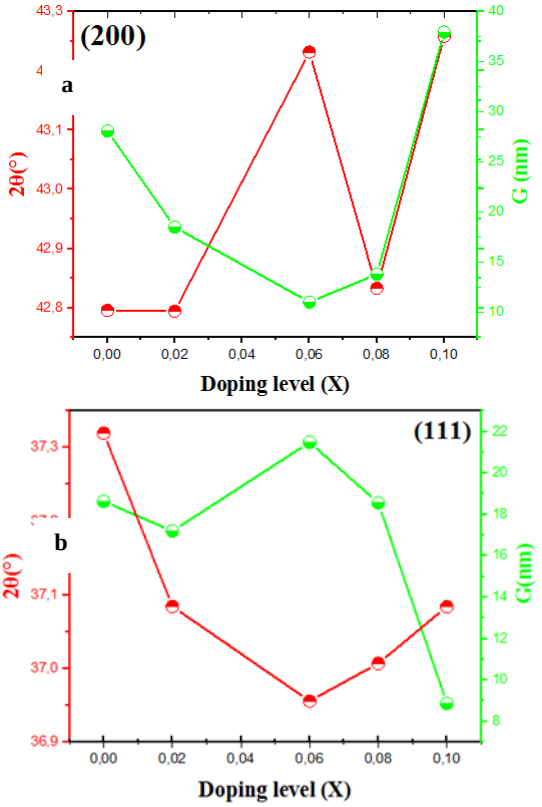

Fig. 2. The variation of crystallite size and diffraction angle of Co doped NiO thin films according to a (111) phase and b (200).

3.2. Optical properties of $Ni_{1-x}Co_xO$ thin films

The Optical characterizations of fabricated $Ni_{1-x}Co_xO$ thin films by doping levels x were performed by measuring the transmittance and absorbance in the wavelength region 300 to 900 nm as it is shown in Figure 3 and 4. As we can see, the value of the average transmission of spray $Ni_{1-x}Co_xO$ thin films is about 70% in the visible region. But for these doping levels x, the region of the absorption edge was located between 330 and 380 nm in comparison with others which are found at 355 and 370 nm [29-30]. It is related region between of the valence band and the conduction band. Figure 4 presents

the variation of absorbance data of thin films of $Ni_{1-x}Co_xO$.

The absorption edge shifts was observed clearly at wavelength shorter than 370nm. The absorption edge shifts of $Ni_{1-x}Co_xO$ thin films increased with the increase of doping levels x. As we can note, the optical property of thin films of $Ni_{1-x}Co_xO$ is affected by doping levels x.

The role of doping levels x on the transmission of thin films of $Ni_{1-x}Co_xO$ was clearly observed on the thin films quality due to the higher transparency. The high transparency was obtained in Co doped NiO thin film with at 8% due to the interstitial site of Co and Ni. That absorbance and the optical band gap energy Eg of fabricated $Ni_{1-x}Co_xO$ thin films were determined by the following relations [31–33]:

$$A = \alpha d = -\ln T \quad (6)$$

$$(Ah\upsilon)^2 = C\left(h\upsilon - E_g\right) \quad (7)$$

where A is the absorbance of fabricated Ni1-xCoxO thin films, α is the absorption coefficient, d is the film thickness, T is the transmission of fabricated $Ni_{1-x}Co_xO$ thin films, C is a constant, hυ is the energy of photon $h\upsilon = \frac{1240}{\lambda(\mathrm{nm})}\ (\mathrm{eV})$ and Eg is the band gap energy of the semiconductor. However, the disorder or Urbach energy (E_u) also was determined by the expression follow [34– 35]:

$$A = A_0 \exp\left(\frac{h\upsilon}{E_u}\right) \quad (8)$$

Where A_0 is a constant, hυ is the energy of photon and E_u is the Urach energy, the tail width of the Urbach energy was used to characterize the order of the defects. The variation of optical band gap energy and Urbach energy of fabricated $Ni_{1-x}Co_xO$ thin films as a function of doping levels x are presented in the Figure 5. The band gap energy was observed a smaller than 3.68 eV. The value of band gap energy decreased and increased with the increase in doping levels from. 3.58 to 3.66 eV.

The diminution in the optical band gap energy value of $Ni_{1-x}Co_xO$ thin films can be illustrated by the effect of quantum confinement due to the diminution in the crystallite size of fabricated $Ni_{1-x}Co_xO$ thin films (see Figure 2). As can be seen in Figure 5, that the value of Urbach energy increased and decreased with the increase in doping levels from 388 to 500 meV. Also, this can be related by the diminution of the crystallite size value (see Figure 2).

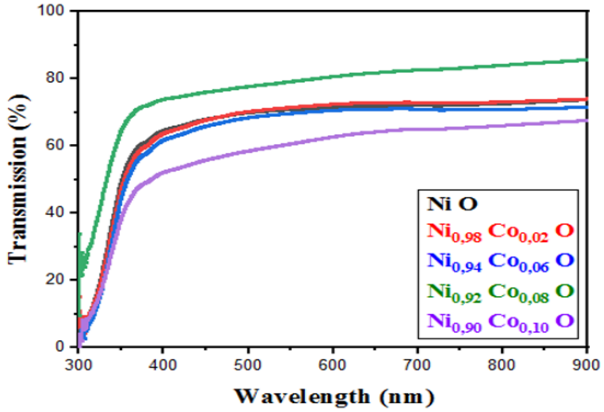

Fig. 3. Transmission spectra of $Ni_{1-x}Co_xO$ thin films as a function of Co doping level.

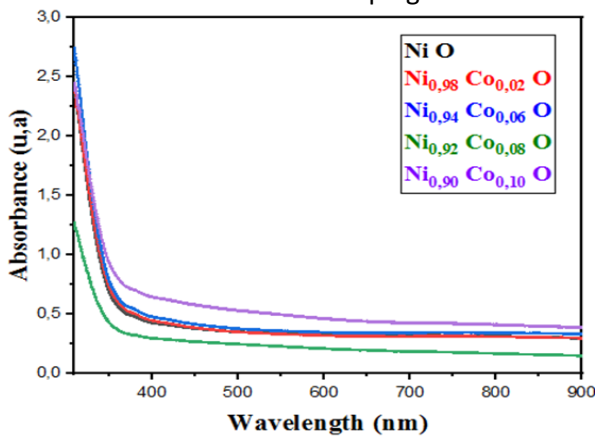

Fig. 4. Absorbance spectra of $Ni_{1-x}Co_xO$ thin films as a function of Co doping level.

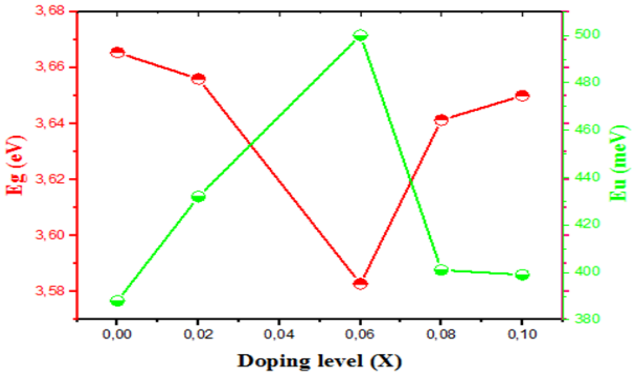

Fig. 5. The variations of optical band gap energy and Urbach energy of Co doped NiO thin films at various doping levels.

3.3. Electrical properties of $Ni_{1-x}Co_xO$ thin films

The four-points probe method was used to determine the electrical conductivity of Ni1-xCoxO thin films, it is based on measuring the sheet resistance of the films as expressed by:

$$R_{sh} = \frac{\pi}{\ln(2)} \cdot \frac{V}{I} \quad (8)$$

Where I is the applied currant I=1 nA and V is the measurement voltage. However, the electrical con-

ductivity σ is also determined by the following equation:

$$\sigma = \frac{1}{d.R_{sh}} \qquad (9)$$

Figure 6 shows the variation of the electrical conductivity of Co doped NiO thin films as a function of Co doping level. As can be seen, the electrical conductivity increases with increasing the Co doping level up to 6 at. % where we obtained a maximum conductivity value which was 0.0015 $(\Omega.cm)^{-1}$. The increase in the conductivity of the $Ni_{1-x}Co_xO$ thin films can be explained by the displacement of the electrons. The latter comes from the Co^{2+} donor ions in the substitutional sites of Ni^{+2} and the formation of the molecular NiCoO existed on the surface. The increase in the conductivity of deposited films after 6 at. % can be related to the increase of the potential barriers, because the introduced atoms are segregated into the grain boundaries [32-33]. The Figures (2, 5 and 6) showed the decrease in the crystallite size, the decrease in optical gab energy, the increase in urbach energy and the increase in electrical conductivity. These results explain the good crystallization of the thin films according to [38– 39– 40– 41].

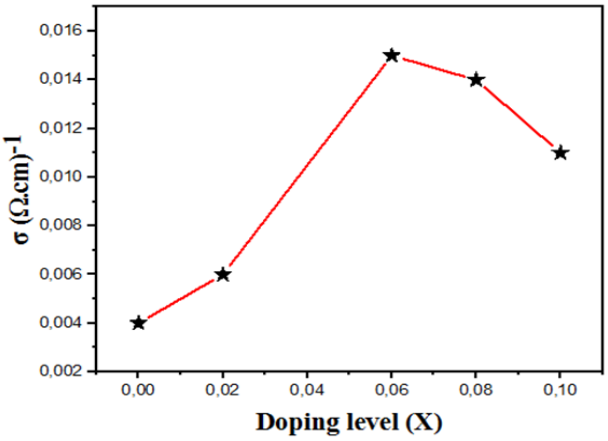

Fig. 6. The electrical conductivity variation of $Ni_{1-x}Co_xO$ thin films as a function of Co doping level.

Conclusion:

In this study, Cobalt doped Nickel Oxide thin films (Co/Ni = 0, 2, 6, 8 and 10 at.%) were successfully deposited on glass substrate by spray pyrolysis technique using Nickel acetate and Cobalt acetate. The $Ni_{1-x}Co_xO$ thin films are transparent in the visible region. The variation of the optical gap energy is between 3.58 and 3.66 eV. The variation of the Urbach energy is between 388 and 500 meV. However, the $Ni_{0.94}Co_{0.06}O$ thin films have many defects with maximum value of urbach energy. The NiO pure thin films have minimum value of urbach energy and maximum value of optical gap energy. The $Ni_{0.94}Co_{0.06}O$ thin films have minimum value of optical gap energy. Also, the $Ni_{0.94}Co_{0.06}O$ thin films have maximum value of the electrical conductivity. The NiO pure thin films have minimum value of the electrical conductivity. The $Ni_{0.94}Co_{0.06}O$ have minimum value of the crystallite size which is 8.9861nm of peak (111) and 11.0152 of peak (200). The NiO pure have maximum value of the crystallite size which is 21.9256 nm of peak (111). The $Ni_{0.90}Co_{0.10}O$ have maximum value of the crystallite size which is 37.9819nm of peak (200). XRD patterns of the $Ni_{1-x}Co_xO$ thin films indicate that films are polycrystalline with cubic structure. The electrical conductivity of deposited films is in the order of $0.01(\Omega.cm)^{-1}$. The Figures (2, 5 and 6) shows the decrease in the crystallite size, the decrease in optical gab energy, the increase in urbach energy and the increase in electrical conductivity. These results explain the good crystallization of the thin films .

References:

[1] V. Verma, M. Katiyar, Thin Solid Films **527**, 369(2013).
[2] S. C. Chen, T. Y. Kuo, Y. C. Lin, H. C. Lin, Thin Solid Films **519**(15), 4944(2011).
[3] R. Sharma, A. D. Acharya, S. B. Shrivastava, M. M. Patidar, M. Gangrade, T. Shripathi, V. Ganesan, Optik **127**(11), 4661(2016).
[4] S. Benramache, M. Aouassa, Journal of Chemistry and Materials Research **5**(6), 119(2016).
[5] S. Dendouga, S. Benramache, S. Lakel, Journal of Chemistry and Materials Research **5**(4), 78(2016).
[6] D. Dini, Y. Halpin, J. G. Vos, E. A. Gibson, Coordination Chemistry Reviews **304–305**, 179(2015).
[7] G. F. Cai, C. D. Gu, J. Zhang, P. C. Liu, X. L. Wang, Y. H. You, J. P. Tu, Electrochimica Acta **87**, 341(2013).
[8] A. C. Nwanya, S. U. I. Offiah, C. Amaechi, S. Agbo, S. C. Ezugwu, B. T. Sone, R. U. Osuji, M. Maaza, F. I. Ezema, Electrochimica Acta **171**,128(2015).
[9] R. Romero, F. Martin, J. R. Ramos-Barrado, D. Leinen, Thin Solid Films **518**(16), 4499(2010).
[10] T. Chtouki, L. Soumahoro, B. Kulyk, H. Bougharraf, B. Kabouchi, H. Erguig, B. Sahraoui,

Optik **128**, 8(2017).
[11] R. J. Deokate, R. S. Kalubarme, C. J. Park, C. D. Lokhande **224**, 378(2017).
[12] Y. Yu, X. Li, Z. Shen, X. Zhang, P. Liu, Y. Gao, T. Jiang, J. Hua, Journal of Colloid and Interface Science **490**, 380(2017).
[13] S. U. Offiah, M. O. Nwodo, A. C. Nwanya, S. C. Ezugwu, S. N. Agbo, P. U. Ugwuoke, R. U. Osuji, M. Malik, F. I. Ezema, Optik **125**, 2905(2014).
[14] S. C. Chen, T. Y. Kuo, Y. C. Lin, S. W. Hsu, H. C. Lin, Thin Solid Films **549**, 50(2013).
[15] X. H. Xia, J. P. Tu, J. Zhang, X. L. Wang, W. K. Zhang, H. Huang, Electrochimica Acta **53**(18), 5721(2008).
[16] I. Castro-Hurtado, J. Herra´n, G. G. Mandayo, E. Castan˜o, Thin Solid Films **520**(3), 947(2011).
[17] C. Zaouche, Y. Aoun, S. Benramache, A. Gahtar, Scientific Bulletin of valahia University materials and mechanics **17**(17), 27(2019).
[18] J. Cao, Z. Wang, R. Wang, S. Liu, T. Fei, L. Wanga, T. Zhang, Materials Chemistry A **3**(10), 5635(2015).
[19] M. AbdurRahman, R. Radhakrishnan, R. Gopalakrishnan, Alloys and Compounds **742**, 421(2018).
[20] A.F. Saleh, Application or Innovation in Engineering & Management **2**(1), 16 (2013).
[21] A. Gahtar, S. Benramache, A. Ammari, A. Boukhachem, A. Ziouche, Inorganic and Nano-Metal Chemistry **52**(1), 112(2022).
[22] A. Gahtar, C. Zaouche, A. Ammari, L. Dahbi, Chalcogenide Letters **20**(5), 377(2023).
[23] N. Beji, M. Reghima, M. Souli, N.K. Turki, Alloys and Compounds **675**, 231 (2016).
[24] S. Chatterjee, S.K. Saha, A.J. Pal, Solar Energy Materials and Solar **147**, 17 (2016).
[25] F.J. Garcia-Garcia, P. Salazar, F. Yubero, A.R. González-Elipe, Electrochimica Acta **201**, 38 (2016).
[26] N. Ali, A. Hussain, R. Ahmed, M.K. Wang, C. Zhao, B. UlHaq, Y.Q. Fu, Renewable and Sustainable Energy Reviews **59**, 726 (2016).
[27] L. Dahbi, C. Zaouche, Y. Benkrima, A. Gahtar, Tobacco Regulatory Science **9**(1), 2819(2023).
[28] S. Benramache, B. Benhaoua, Superlattices and Microstructures **52**(16), 1062 (2012).
[29] O. Bayram, E. Sener, E. İgman. O. Simsek, Journal of Materials Science Materials in Electronics **30**, 3452(2019).
[30] C. Zaouche, S. Benramache, International Journal of Advanced Multidisciplinary Research and Studies **3**(5), 68(2023).
[31] A. Diha, S. Benramache, B. Benhaoua, Optik **172**, 832(2018).
[32] S. Benramache, Y. Aoun, S. Lakel, H. Mourghade, R. Gacem, B. Benhaoua, Journal of Nano- and Electronic Physics **10**, 06032(2018).
[33] C. Zaouche, L. Dahbi, S. Benramache, A. Harouache, Y. Derouiche, M. Kharroubi, H. A. Haslouk, M. A. A. Banalhag, H. M. Alkhoja, Journal of Ovonic Research **19**(2), 197(2023).
[34] W. Daranfed, M. S. Aida, A. Hafdallah, H. Lekiket, Thin Solid Films **518**, 1082(2009).
[35] A. Gahtar, S. Benramache, C. Zaouche, A. Boukacham, A. Sayah, ADVANCES IN MATERIALS SCIENCE **20**(3), 36(2020).
[36] S. Benramache, B. Benhaoua, F. Chabane, Journal of Semiconductors **33**(9), 093001(2012).
[37] C. Zaouche, S. Benramache, A. Gahtar, Biomedical Journal of Scientific Technical Research **52**(3), 43761(2023).
[38] C. Zaouche, A. Gahtar, S. Benramache, Y. Derouiche, M. Kharroubi, A. Belbel, C. Maghni, L. Dahbi, Digest Journal of Nanomaterials and Biostructures **17**(4), 1453(2022).
[39] S. Benramache, Y. Aoun, A. Charef, B. Benhaoua, S. Lake, Inorganic and Nano-Metal Chemistry **49**, 177(2019).
[40] M. Othmane, A. Attaf, H. Saidi, F. Bouaichi, N. Lehraki, M. Nouadji, M. Poulain, S. Benramache, International Journal of Nanoscience **15**, 1650007(2015).
[41] A. Gahtar, A. Benali, S. Benramache, C. Zaouche, Chalcogenide Letters **19**(2), 103(2022).